

Water in lunar anorthosites and evidence for a wet early Moon

Hejiu Hui^{1*}, Anne H. Peslier^{2,3}, Youxue Zhang⁴ and Clive R. Neal¹

The Moon was thought to be anhydrous since the Apollo era¹, but this view has been challenged by detections of water on the lunar surface²⁻⁴ and in volcanic rocks⁵⁻⁹ and regolith¹⁰. Part of this water is thought to have been brought through solar-wind implantation^{2-4,7,10} and meteorite impacts^{2,3,7,11}, long after the primary lunar crust formed from the cooling magma ocean^{12,13}. Here we show that this primary crust of the Moon contains significant amounts of water. We analysed plagioclase grains in lunar anorthosites thought to sample the primary crust, obtained in the Apollo missions, using Fourier-transform infrared spectroscopy, and detected approximately 6 ppm water. We also detected up to 2.7 ppm water in plagioclase grains in troctolites also from the lunar highland upper crust. From these measurements, we estimate that the initial water content of the lunar magma ocean was approximately 320 ppm; water accumulating in the final residuum of the lunar magma ocean could have reached 1.4 wt%, an amount sufficient to explain water contents measured in lunar volcanic rocks. The presence of water in the primary crust implies a more prolonged crystallization of the lunar magma ocean than a dry moon scenario and suggests that water may have played a key role in the genesis of lunar basalts.

Dissolved water in silicates can alter their structure, and hence significantly change their physical and chemical properties¹⁴⁻¹⁷, which can further influence geologic processes. One of the most important conclusions resulting from the Apollo and Luna missions was that no water was detected in returned samples or at the surface of the Moon¹. The Moon was thought to have lost its volatiles as it formed from ejecta of the impact of a Mars-size planetesimal with the proto Earth, the favoured Moon formation scenario¹⁸, and during degassing of an early planet-wide magma ocean^{12,13}. This notion has been included in most geophysical and geochemical models of formation and evolution of the Moon^{12,18}. The view of a dry lunar interior, however, has been challenged by recent discoveries of water in picritic glass beads⁵, apatites⁶⁻⁸ and olivine melt inclusions⁹, which were facilitated by the improvements of the analytical detection limit of hydrogen. Indigenous water is suggested to be heterogeneously distributed in the lunar interior and some parts of lunar mantle may contain as much water as Earth's upper mantle^{5,9}. Hydrogen isotopic compositions of apatites in mare basalts have been interpreted to indicate a hybrid source of the water, that is, a combination of lunar mantle, comets and solar-wind protons⁷. The chlorine isotope compositions in the lunar pyroclastic deposits, however, have been interpreted as suggesting an essentially anhydrous lunar interior¹⁹. It has been further suggested using magma ocean crystallization modelling that

the water content of the bulk lunar magma ocean (LMO) was less (possibly far less) than 100 ppm and water was later added during mantle cumulate overturn or through impacts¹¹.

Here we have measured water in primary products of the LMO, thereby bypassing the processes of later addition of water to the Moon through impact events or during mantle overturn as suggested by previous studies^{7,11}. These data are used to estimate the water content of the Moon's interior at the time of the magma ocean, as well as that of the mare magma source regions. So far, ferroan anorthosite (FAN) is the only available lithology that is believed to be a primary product of the LMO (refs 12,13). It is generally accepted that plagioclase, after crystallization, floated in the magma ocean and formed FAN as the original crust of the Moon¹². Therefore, any indigenous water preserved in pristine FAN was partitioned from the magma ocean. Fourier-transform infrared spectroscopy (FTIR) was used to measure water contents in plagioclases of FANs 15415,238 and 60015,787 (see Supplementary Information S1). Both these samples have >98 vol% of plagioclase with anorthite contents >96%. To assess the water inventory in the lunar highland upper crust, nominally anhydrous minerals in troctolite 76535,164 (see Supplementary Information S1) were also analysed using FTIR. Troctolite, an olivine-rich end member of the Mg suite that composes about half of the highland upper crust²⁰, is thought to be derived from the magma ocean crystallization products, but its detailed origin is under debate²⁰.

The mineral grains allocated for this study are from the interior portion of each individual rock. Therefore, potential hydrogen implanted by solar wind¹⁰ was avoided because direct solar implantation is limited to 0.2 μm depth from the sample surfaces²¹, and even though micrometeorite gardening and melting can transfer OH to some depth on the basis of a recent study of lunar agglutinitic glasses¹⁰, such OH is in glasses from impact remelting, not pristine minerals. Layers of tens to a few hundred micrometres in thickness on both sides of each grain were also removed in the preparation of doubly polished parallel surfaces for FTIR analyses (see Methods), which further ensured the removal of any layer affected by solar implantation. Infrared spectra of plagioclase from FAN 15415,238 and 60015,787 are characterized by a small wide absorption band in the O–H region (Fig. 1 and Supplementary Fig. S2) that resembles those observed in terrestrial plagioclases^{22,23}. This broad band ($\sim 3,700$ to $\sim 3,100$ cm^{-1}) is interpreted as absorption by structural O–H bond vibrations in plagioclase for two reasons. First, one of our doubly polished grains of 15415 was heated to 1,000 °C for 24 h in a high-purity N_2 atmosphere at the University of Michigan and then cleaned with the same procedure (see Methods). The band is strongly diminished in the heated sample, demonstrating that

¹Department of Civil and Environmental Engineering and Earth Sciences, University of Notre Dame, Notre Dame, Indiana 46556, USA, ²Jacobs Technology, ESCG, Mail Code JE23, Houston, Texas 77058, USA, ³ARES, NASA-Johnson Space Center, Mail Code KR, Houston, Texas 77058, USA, ⁴Department of Earth and Environmental Sciences, University of Michigan, Ann Arbor, Michigan 48109, USA. *e-mail: hhui@nd.edu.

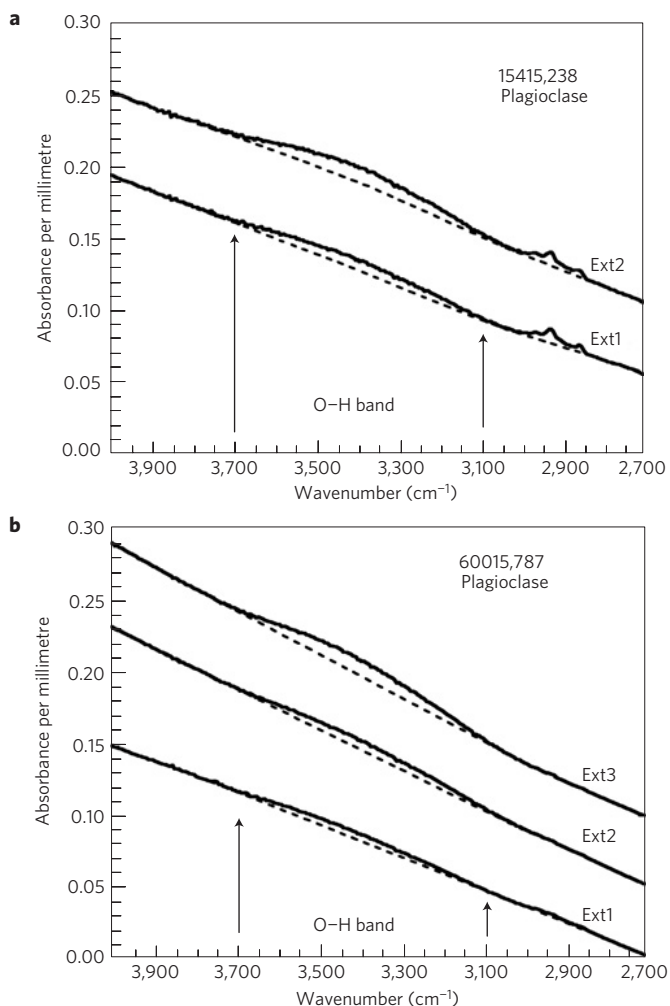


Figure 1 | Representative polarized FTIR spectra of plagioclase from FANs. a, b, Spectra for 15415,238 (a) and 60015,787 (b) at mutually perpendicular orientations (Ext1, Ext2 and Ext3: optical extinction directions 1, 2 and 3) are normalized to 1 mm and shifted vertically for comparison. The dashed line indicates the baseline position used for water content estimations. The narrow peaks ($3,000\text{--}2,800\text{ cm}^{-1}$) most probably come from organic contamination on the mineral surface during sample preparation^{22,23}. The spectra with the same label (for example, Ext1) for different crystals were not taken at the same crystal orientation relative to the mineral crystallographic axis.

dehydration occurred (Fig. 2). Second, the anisotropy of the O–H absorption band height or absorbance area during rotation of the infrared polarizer relative to the plagioclase crystals, and the 90° interval between maximum and minimum (Supplementary Fig. S4) demonstrate that this band (Fig. 1 and Supplementary Fig. S2) cannot be caused by water in minute melt or fluid inclusions²³ or by contamination during sample preparation. Furthermore, O–H absorbance area does not seem related to the degree of plagioclase fracturing that was probably produced during impact. Total integrated absorption areas of the OH bands (A_{tot} in cm^{-2}) along three mutually perpendicular directions (see Supplementary Information S2) were converted to water contents ($C_{\text{H}_2\text{O}}$ in parts per million by weight of H_2O) using the Beer–Lambert law in the form $C_{\text{H}_2\text{O}} = A_{\text{tot}}/I'$, where I' is the calibrated specific integral absorption coefficient ($15.3 \pm 0.7\text{ ppm}^{-1}\text{ cm}^{-2}$ for feldspars²²). Although infrared absorbances are typically reproducible between different laboratories²⁴, we nonetheless verified the accuracy of our measurement by analysing an external standard, the plagioclase used

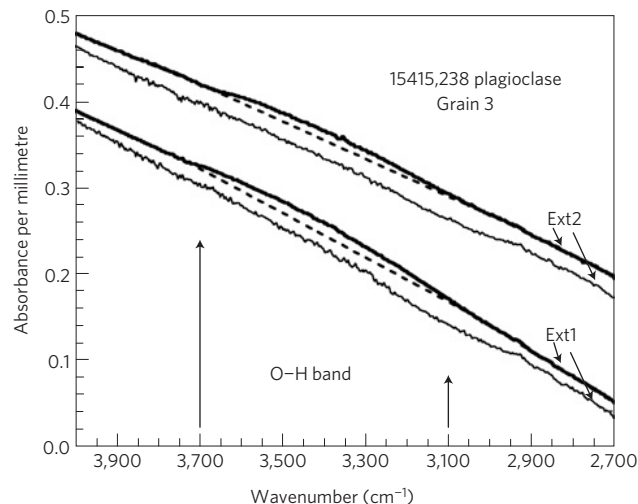


Figure 2 | FTIR spectra of plagioclase from 15415,238 before and after heating at $1,000^\circ\text{C}$ for 24 h. FTIR analyses were performed on the sample before (upper thick curve with the dashed baseline used for water content estimation) and after the heating experiment (lower thin curve) at the same orientations of the sample relative to the polarizer (Ext1 and Ext2, respectively). The diminished band ($\sim 3,700$ to $\sim 3,100\text{ cm}^{-1}$) in the spectrum of the heated sample demonstrates that dehydration occurred. The band in the untreated sample is due to absorption of O–H bond vibration, and not an artefact in the baseline.

for the absorption coefficient calibration²², GRR1968. The total absorbance area of spectra at three mutually perpendicular directions and with sample thickness normalized to 1 cm is $1,712\text{ cm}^{-2}$, differing from that of $1,688\text{ cm}^{-2}$ in ref. 22 by 1.4% relative, thereby verifying inter-laboratory reproducibility. The water contents in plagioclases are $\geq 5.0\text{ ppm H}_2\text{O}$ by weight (grain Pl3) for 15415,238 and 6.4 ppm for 60015,787 (Supplementary Table S1). Note that there could be a systematic error in the calibration for plagioclase, which would act to underestimate water contents calculated using this calibration (see Supplementary Information S2).

The water partition coefficient between plagioclase and silicate melt is not well constrained (see Supplementary Information S3), which is a main source of uncertainty in the following discussion. Using a partition coefficient of 0.004 between plagioclase and silicate melt²⁵, the water content of a melt in equilibrium with 60015 plagioclase is calculated to be $\sim 1,600\text{ ppm H}_2\text{O}$. Co-crystallized pyroxene cumulates should contain $\sim 11\text{ ppm H}_2\text{O}$ using a partition coefficient of 0.007 between pyroxene and silicate melt²⁶. About 1,600 ppm represents the amount of water in the residual melt of the magma ocean, when floating plagioclase was forming the original lunar crust. At that point, approximately 80 vol% of the LMO is thought to have been solidified¹². Using this degree of crystallization, the amount of water in the parental magma of FAN 60015, that is, in the initial magma ocean, is inferred to be $\sim 320\text{ ppm H}_2\text{O}$ (Fig. 3). The first crystallized olivine cumulate in the LMO could have $\sim 0.6\text{ ppm}$ of water using a partition coefficient of 0.002 between olivine and silicate melt²⁷, which is much higher than $\sim 90\text{ ppb}$ of water in the lunar mantle inferred from Cl isotope studies¹⁹. As crystallization of the LMO continued, volatiles and other incompatible trace elements became enriched in the magma ocean residuum. On the basis of the LMO model¹², the final 2 vol% of the magma ocean residuum (urKREEP) that may be the source of the potassium, rare-earth and phosphorus (KREEP)-rich lithologies unique to the Moon potentially could have had as much as $\sim 1.4\text{ wt\%}$ of water. This is an order of magnitude higher than the thousands of parts per million maximum suggested previously¹¹, and also 1.5 orders of magnitude higher than 850–1,100 ppm in

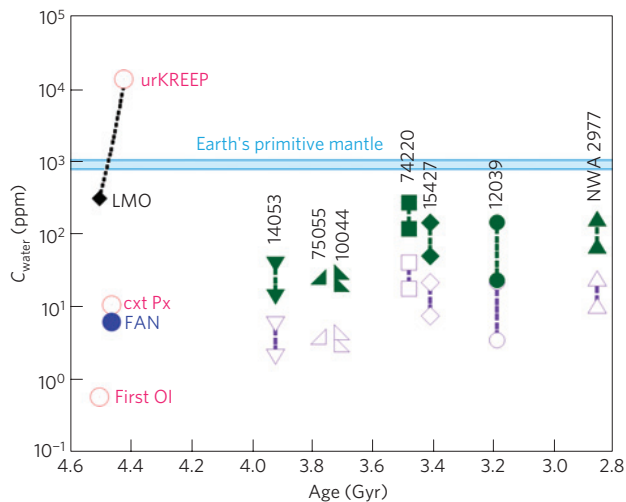


Figure 3 | Water contents in LMO products and mantle sources of basalts through time. Model ages are used for primary magma ocean products^{12,13} and isochron ages for the basalts (Supplementary Table S2). Water contents of the initial magma ocean (LMO), the first crystallized olivine cumulate (first OI), co-crystallized pyroxene cumulate (cxt Px) and urKREEP were estimated from the water content measured in FAN plagioclases. The black dashed line from LMO to urKREEP shows the water content evolution in magma ocean residua. The water contents of mantle sources with isochron ages <4.0 Gyr were calculated assuming 20% (green) or 3% partial melting (purple; Supplementary Table S2).

Earth's primitive mantle²⁸ (Fig. 3). This implies that the LMO crystallization products could have spanned a wide range of water contents, from <1 ppm to ~1.4 wt% (Fig. 3). After the LMO solidification, these materials are thought to have undergone gravitational overturn driven by density difference²⁹. Overturned lunar cumulate mantle provided the source regions for mare basalts^{12,29}. Even assuming 20% of partial melting of the source regions of mare basalts in which water was detected^{5–9}, calculated water contents of their source regions are still well within the range of those we calculated for the primary magma ocean products inferred from water content in plagioclase from FANs (Fig. 3).

Even a small amount of water can change the liquid line of descent of melt and suppress crystallization of plagioclase relative to olivine and clinopyroxene, such as in mid-ocean ridge basalts¹⁵. Therefore, the amount of water we calculated could affect the LMO crystallization dynamics, especially for the last few tens of volume per cent of magma ocean residuum. The depression of the liquidus due to increased water contents would also prolong the crystallization of the LMO and potentially explain an extraordinarily young age ($4,360 \pm 3$ Myr) for FAN 60025 (ref. 30) in the framework of a magma ocean model. Note that an alternative explanation of the young age has been suggested by challenging the existence of a global magma ocean³⁰. Even if the latter argument is correct, the measured water concentration in plagioclase can still be used to infer water contents of parental magmas of cumulates that formed the earliest lunar crust. Moreover, the relatively high abundance of water (~1.4 wt%) in urKREEP can significantly change its physical properties, such as lowering density¹⁶ and viscosity¹⁷, which could affect the dynamics of magma ocean cumulate overturn²⁹. In summary, the variable amounts of water in urKREEP and earlier cumulates (Fig. 3) could play a critical role on the genesis of lunar basalts, in which indigenous water has been recently discovered^{5–9}, in a similar way to the role of water in terrestrial oceanic mantle melting regimes¹⁴.

Intrinsic water was also detected in plagioclase of troctolite 76535,164 (Fig. 4 and Supplementary Fig. S3). The minimum

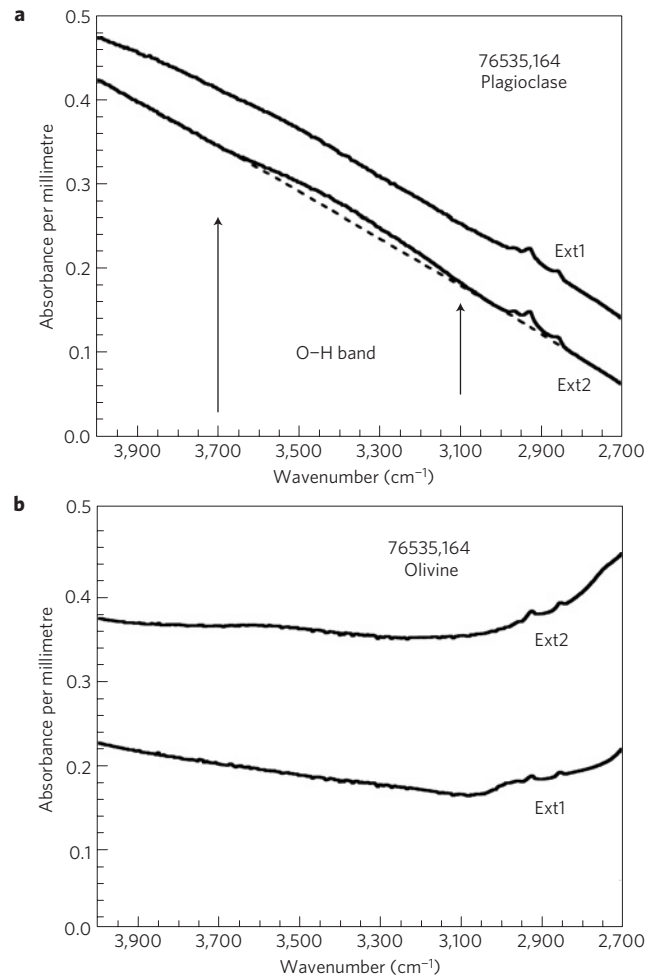


Figure 4 | Representative polarized FTIR spectra of troctolite 76535,164. **a, b,** Spectra of plagioclase (**a**) and olivine (**b**) at two mutually perpendicular orientations (Ext1 and Ext2) are normalized to 1 mm and shifted vertically for comparison. The dashed line indicates the baseline position used to calculate water concentrations (see Supplementary Information S2). No obvious OH bands are observed in the spectra taken with orientation Ext1 of plagioclase or in any of the olivine spectra. The narrow peaks between 3,000 and 2,800 cm^{-1} most probably come from organic contamination on the mineral surface during sample preparation^{22,23}.

water contents vary from 0.8 to 2.7 ppm (Pl1 of 76535,164) (Supplementary Table S1). No O–H absorption band has been observed in a 1.055-mm-thick olivine from this troctolite (Fig. 4), implying a H_2O content of <1 ppm. The fact that plagioclase is more hydrous than olivine is consistent with the H_2O partition coefficient between olivine and melt being smaller than that between plagioclase and melt^{25,27}. The minimum whole-rock water content of troctolite 76535 is ~2 ppm on the basis of its mineral modal abundance, which is lower than that calculated for the initial magma ocean from our FAN data.

The presence of indigenous water in FAN and troctolite suggests that the highland upper crust is not anhydrous. Considering the distributions of two major lithologies (FAN and Mg suite) in the highland upper crust²⁰ and assuming that the results for 60015 (~6 ppm) and 76535 (~2 ppm) are representative of FANs and the Mg suite, respectively, the upper crust may contain ~4 ppm of indigenous water. Incidentally, trace amounts of water/hydroxyl have been detected in the lunar highlands surface by various spacecrafts, although lack of hydroxyl reflectance calibration meant that it could not be quantified³. Hence, another implication of

the results presented here is that the water measured in lunar highland lithologies may contribute a significant portion of the water detected by spacecraft.

Methods

Plagioclase grains from FANs 15415,238 and 60015,787, and plagioclase and olivine grains from one troctolite 76535,164 were analysed by FTIR to determine water contents. Each mineral grain was embedded in crystal bond and a doubly polished section was prepared manually using sandpaper and alumina powder (down to 1 µm). The grain was not polished at any orientation relative to the crystallographic axis (that is, with polished surface perpendicular to the optic normal, acute bisectrix or obtuse bisectrix directions). Instead a mineral section of random orientation was made as thick as possible to get maximum infrared signal for O–H bond vibrations with a relatively good spectrum signal–noise ratio. One plagioclase grain of 60015 was large enough to be polished into a mineral cube with two sets of polished mutually perpendicular surfaces. The polished grains were cleaned successively with acetone, ethanol, deionized water and CH₂Cl₂ in an ultrasonic bath. A plagioclase (GRR1968) previously analysed by another laboratory²² was also polished into a cube using the same procedure to check for inter-laboratory reproducibility. The thickness of each grain was measured using a Mitutoyo digital micrometer. Before FTIR analysis of each grain, the sample chamber was flushed with N₂ for at least an hour.

Polarized FTIR spectra with wavenumbers from 7,800 to 600 cm⁻¹ were collected using a Hyperion 3000 microscope attached to a Bruker Vertex 70 FTIR spectrometer at the Astromaterial and Research Exploration Science (ARES) directorate of the NASA-Johnson Space Center. The standard mercury cadmium telluride detector and KBr beam splitter were used during FTIR analysis, as well as a Zn–Se wire-grid polarizer. Aperture size from 255 × 255 µm to 425 × 425 µm (mainly 340 × 340 µm) during each analysis was chosen on the basis of the grain size. During each analysis, 256 scans were performed for each infrared measurement under a nitrogen environment, to minimize interference from atmospheric water vapour. A new background was collected before each infrared measurement on a new grain or the same grain using a different polarizing angle. Polarized infrared spectra (wave numbers from 9,000 to 1,500 cm⁻¹) were also acquired using an AutoImage microscope on a Perkin-Elmer Spectrum GX FTIR spectrometer at the University of Michigan. A near-infrared source, CaF₂ beam splitter, KRS-5 infrared wire-grid polarizer, mercury cadmium telluride detector and N₂ gas purge and an aperture size of 340 × 340 µm were used during these FTIR analyses. The spectra from two different FTIR are consistent with each other.

Received 21 June 2012; accepted 17 January 2013; published online 17 February 2013

References

- Lucey, P. *et al.* Understanding the lunar surface and space–Moon interactions. *Rev. Mineral. Geochem.* **60**, 83–219 (2006).
- Clark, R. N. Detection of adsorbed water and hydroxyl on the Moon. *Science* **326**, 562–564 (2009).
- Pieters, C. M. *et al.* Character and spatial distribution of OH/H₂O on the surface of the Moon seen by M³ on Chandrayaan-1. *Science* **326**, 568–572 (2009).
- Sunshine, J. M. *et al.* Temporal and spatial variability of lunar hydration as observed by the deep impact spacecraft. *Science* **326**, 565–568 (2009).
- Saal, A. E. *et al.* Volatile content of lunar volcanic glasses and the presence of water in the Moon's interior. *Nature* **454**, 192–195 (2008).
- Boyce, J. W. *et al.* Lunar apatite with terrestrial volatile abundances. *Nature* **466**, 466–469 (2010).
- Greenwood, J. P. *et al.* Hydrogen isotope ratios in lunar rocks indicate delivery of cometary water to the Moon. *Nature Geosci.* **4**, 79–82 (2011).
- McCubbin, F. M. *et al.* Nominally hydrous magmatism on the Moon. *Proc. Natl Acad. Sci. USA* **107**, 11223–11228 (2010).
- Hauri, E. H., Weinreich, T., Saal, A. E., Rutherford, M. C. & Van Orman, J. A. High pre-eruptive water contents preserved in lunar melt inclusions. *Science* **333**, 213–215 (2011).
- Liu, Y. *et al.* Direct measurement of hydroxyl in the lunar regolith and the origin of lunar surface water. *Nature Geosci.* **5**, 779–782 (2012).
- Elkins-Tanton, L. T. & Grove, T. L. Water (hydrogen) in the lunar mantle: Results from petrology and magma ocean modelling. *Earth Planet. Sci. Lett.* **307**, 173–179 (2011).
- Shearer, C. K. *et al.* Thermal and magmatic evolution of the Moon. *Rev. Mineral. Geochem.* **60**, 365–518 (2006).
- Norman, M. D., Borg, L. E., Nyquist, L. E. & Bogard, D. D. Chronology, geochemistry, and petrology of a ferroan noritic anorthosite clast from Descartes breccia 67215: Clues to the age, origin, structure, and impact history of the lunar crust. *Meteorol. Planet. Sci.* **38**, 645–661 (2003).
- Asimow, P. D. & Langmuir, C. H. The importance of water to oceanic mantle melting regimes. *Nature* **421**, 815–820 (2003).
- Danyushevsky, L. V. The effect of small amounts of H₂O on crystallization of mid-ocean ridge and backarc basin magmas. *J. Volcanol. Geotherm. Res.* **110**, 265–280 (2001).
- Ochs, F. A. III & Lange, R. A. The density of hydrous magmatic liquids. *Science* **283**, 1314–1317 (1999).
- Hui, H. & Zhang, Y. Toward a general viscosity equation for natural anhydrous and hydrous silicate melts. *Geochim. Cosmochim. Acta* **71**, 403–416 (2007).
- Canup, R. M. & Asphaug, E. Origin of the Moon in a giant impact near the end of the Earth's formation. *Nature* **412**, 708–712 (2001).
- Sharp, Z. D., Shearer, C. K., McKeegan, K. D., Barnes, J. D. & Wang, Y. Q. The chlorine isotope composition of the Moon and implications for an anhydrous mantle. *Science* **329**, 1050–1053 (2010).
- Hess, P. C. Petrogenesis of lunar troctolites. *J. Geophys. Res.* **99**, 19083–19093 (1994).
- Keller, L. P. & McKay, D. S. The nature and origin of rims on lunar soil grains. *Geochim. Cosmochim. Acta* **61**, 2331–2341 (1997).
- Johnson, E. A. & Rossman, G. R. The concentration and speciation of hydrogen in feldspars using FTIR and ¹H MAS NMR spectroscopy. *Am. Mineral.* **88**, 901–911 (2003).
- Johnson, E. A. & Rossman, G. R. A survey of hydrous species and concentrations in igneous feldspars. *Am. Mineral.* **89**, 586–600 (2004).
- Behrens, H., Romano, C., Nowak, M., Holtz, F. & Dingwell, D. B. Near-infrared spectroscopic determination of water species in glasses of the system MAlSi₃O₈ (M = Li, Na, K): An interlaboratory study. *Chem. Geol.* **128**, 41–63 (1996).
- Johnson, E. A. Water in nominally anhydrous crustal minerals: Speciation, concentration, and geologic significance. *Rev. Mineral. Geochem.* **62**, 117–154 (2006).
- O'Leary, J. A., Gaetani, G. A. & Hauri, E. H. The effect of tetrahedral Al³⁺ on the partitioning of water between clinopyroxene and silicate melt. *Earth Planet. Sci. Lett.* **297**, 111–120 (2010).
- Hauri, E. H., Gaetani, G. A. & Green, T. H. Partitioning of water during melting of the Earth's upper mantle at H₂O-undersaturated conditions. *Earth Planet. Sci. Lett.* **248**, 715–734 (2006).
- Palme, H. & O'Neill, H. St. C. Cosmochemical estimates of mantle composition. *Treatise Geochem.* **2**, 1–38 (2004).
- Spera, F. J. Lunar magma transport phenomena. *Geochim. Cosmochim. Acta* **56**, 2253–2265 (1992).
- Borg, L. E., Connelly, J. N., Boyet, M. & Carlson, R. W. Chronological evidence that the Moon is either young or did not have a global magma ocean. *Nature* **477**, 70–72 (2011).

Acknowledgements

This work was supported by NASA (NNX11AH48G to H.H. and NNX10AH74G to Y.Z.). We thank the Apollo sample curators for allocating us the samples and G. Rossman for providing an aliquot of plagioclase GRR1968. H.H. thanks Y. Chen for technical assistance on heating experiments and electron microprobe analyses, and D. Draper and the LPI for help to access the JSC facility. This manuscript was greatly improved by the suggestions and comments of E. A. Johnson.

Author contributions

H.H. conceived this study and performed the analyses and experiments. Y.Z. provided the terrestrial plagioclase grains. A.H.P. and Y.Z. assisted in experiments and FTIR analyses. H.H., A.H.P., Y.Z. and C.R.N. discussed the data and wrote the paper.

Additional information

Supplementary information is available in the [online version of the paper](#). Reprints and permissions information is available online at www.nature.com/reprints. Correspondence and requests for materials should be addressed to H.H.

Competing financial interests

The authors declare no competing financial interests.

Water in lunar anorthosites and evidence for a wet early Moon

Hejiu Hui¹, Anne H. Peslier^{2,3}, Youxue Zhang⁴, Clive R. Neal¹

¹ Department of Civil & Environmental Engineering & Earth Sciences, University of Notre Dame, Notre Dame, IN 46556

² Jacobs Technology, ESCG, Mail Code JE23, Houston, TX 77058

³ ARES, NASA-Johnson Space Center, Mail Code KR, Houston, TX 77058

⁴ Department of Earth and Environmental Sciences, University of Michigan, Ann Arbor, MI 48109

Supplementary Information

1. Description of Ferroan Anorthosites 15415 and 61005, and Troctolite 76535

Ferroan anorthosite 15415 is one of the best known rocks of the Apollo collection, and is popularly called the “Genesis Rock” because the astronauts thought they had a piece of the Moon’s primordial crust. It was collected on the rim of Apur Crater during the Apollo 15 mission¹. Rock 15415 is a pristine coarse-grained, unbrecciated anorthosite composed of 99 vol.% calcic plagioclase (An_{96.9})². The plagioclase is homogenous with the variation of anorthite content being within 1 mol.%². Besides plagioclase, accessory augite and traces of orthopyroxene and ilmenite have been observed³. No crystallization age has been determined for 15415^{4,5} but ages for ferroan anorthosites range from 4.29 to 4.56 Ga⁶. This rock has experienced multiple episodes of shattering and impact³. However, the low abundance of siderophile elements supports the chemical pristinity of this ferroan anorthosite⁷. The aliquot of 15415,238 allocated to us is composed of plagioclase grains from the interior portion of this rock. These mineral grains are anhedral, full of fractures and tiny (<50 μm) mineral inclusions (Fig. S1). Melt inclusions are absent.

Rock 60015 is a highly shocked ferroan anorthosite, which was collected near the Lunar Module during the Apollo 16 mission. The rock is covered by a rind of thick black glass⁸. The interior consists almost entirely of anorthitic plagioclase (>98 vol.%), with accessory pyroxene (orthopyroxene and augite, ~1.3 vol.%) and trace amount of ilmenite (~0.1 vol.%)⁸. Plagioclase is homogenous (An_{96.4-97.1})⁸. Metallic iron detected in the interior portion has low concentrations of Ni and Co⁹ and the rock has extremely low concentrations of siderophile elements¹⁰, which suggests there was no meteoritic contamination at least for the interior portion^{9,11}. No crystallization age has been determined for 60015¹². Our aliquot from 60015,787 obtained from the Lunar Samples Curation was a large (~3 mm) plagioclase grain from the interior portion. This mineral grain is anhedral, full of fractures and tiny mineral inclusions. A few bubble-like inclusions were also observed, which may indicate that shock-induced temperature was high enough to initiate partial melting⁸.

Troctolite 76535 is a coarse-grained plutonic rock, collected at Station 6 during the Apollo 17 mission. It has an equilibrated texture, mainly composed of olivine (60 vol.%), anorthitic plagioclase (35 vol.%), and orthopyroxene (5 vol.%)¹³. Olivine is very homogeneous (Fo_{87.3}) as is plagioclase (An_{96.2}) and orthopyroxene (En_{84.1}Wo_{0.9})¹³. Other

minor phases observed in this rock include augite, spinel, apatite, merrillite, metal and baddeleyite¹³. This rock has very low abundance of siderophile elements¹⁴, which suggests it is chemically pristine. Isotopic U-Th-Pb studies yielded an age of 4.236 ± 0.015 Ga¹⁵, which is consistent with the Sm-Nd isotopic age of 4.26 ± 0.06 Ga¹⁶, but is younger than the Rb-Sr isotopic age of 4.61 ± 0.07 Ga¹⁷. The aliquot 76535,164 allocated to us consists of plagioclase and olivine grains from the interior portion of 76535. Both olivine and plagioclase contain abundant acicular to rounded opaque inclusions. In general, the plagioclase grains contain more fractures than the olivine grains.

2. Quantitative determination of water contents

Quantitative water estimations in nominally anhydrous biaxial minerals by FTIR are based on the total integrated absorption intensities in the OH region, which is typically taken as the sum of the integrated absorption intensities of polarized spectra in three principal optical orientations (i.e., perpendicular to the optic normal, acute bisectrix or obtuse bisectrix directions) of the mineral¹⁸. However, it was not possible to prepare our lunar crystals with polished faces oriented in the three principal optic orientations. On the other hand, the sum of the integrated absorption intensities of any three mutually perpendicular directions can also be used^{19,20}. Even then it is still difficult to get two sets of mutually perpendicular surfaces in these randomly oriented highland mineral grains because they tend to break along fractures. Four large plagioclase grains of 15415, and four large plagioclase grains and two olivine grains in 76535 were doubly polished to thick sections for FTIR analysis (Table S1). Only one plagioclase grain of 60015 could be polished into a cube with two sets of mutually perpendicular surfaces. The fractures observed from the petrographic microscope, especially those extended to polished surfaces and the large ones within crystal were avoided during FTIR analyses when possible.

Infrared spectra of plagioclase from FAN 15415,238 and 60015,787, and troctolite 76535,164 are characterized by a small wide absorption band in the O-H region (Figs. 1, 3, S2 and S3) and resemble those observed in terrestrial plagioclases from the literature^{19,20}. Several tests were made to prove that the small band is due to intrinsic OH vibration absorption and not an artifact of the baseline. Plagioclase Grain 3 of FAN 15415,238 was heated at 1000 °C for 24 hours in a Deltech furnace in a purified N₂ environment and then cleaned with the same procedure used for untreated samples. This sample was analyzed with the same FTIR setting before and after heating. The spectra of heated sample is essentially free of the small OH band compared with that of untreated sample (Fig. 2), indicating that the O-H bands observed in IR spectra of lunar plagioclase (Figs. 1, 4, S2 and S3) are caused by O-H bond vibrations, and that the water was lost during the heating experiment. To test that the observed band is structural OH, IR spectra were taken on the same spot by varying the polarizer direction (E-vector direction). The anisotropy of the OH absorption band area during rotation of the infrared polarizer in plagioclase (Fig. S4) demonstrates that the bands (Figs. 1, 4, S2 and S3) are caused by structural hydroxyl species in the plagioclase grains and not by water in melt inclusions²⁰. These tests also demonstrate that the OH absorption band is unlikely caused by contamination during sample preparation. No absorption bands were observed at 5240 cm^{-1} (Fig. S5), which would have indicated the presence of molecular water if

sufficient amounts of water were incorporated in plagioclase. Consequently, the wide absorption bands ($\sim 3700 - \sim 3100 \text{ cm}^{-1}$; Figs. 1, 4, S2 and S3) are caused by structural hydroxyl species in plagioclase^{20,21}. No OH band was detected in olivine spectra of 76535 (Fig. 4). Using the Omnic[®] software, all the spectra were normalized to 1 cm thickness and the baseline for each spectrum was manually drawn following the procedure described by Johnson and Rossman^{19,20}. Our results indicate that OH is roughly homogeneously distributed within each plagioclase grain for FAN 15415 and 60015 (Table S1). Only one aggregate plagioclase grain (P11) from troctolite 76535 has detectable OH bands in its spectra. It may be because this grain is an aggregate that the spectra from different locations have variable OH band intensities (Figs. 4 and S3).

The absorption intensity in the OH region was determined by integrating the area above the manually drawn baseline (between 3700 and 3100 cm^{-1} for plagioclase). The overall absorption band area represents the sum of that for different mutually perpendicular orientations (Table S1). A piece of plagioclase crystal GRR1968, which was used to calibrate the specific integral absorption coefficient of water in plagioclase by Johnson and Rossman¹⁹, was also analyzed along three mutually perpendicular directions in this study for comparison. The total IR band area obtained from our own analysis and for a sample thickness normalized to 1 cm is 1712 cm^{-2} , which agrees with the result (1688 cm^{-2}) in Johnson and Rossman¹⁹ with 1.4% relative difference. Total absorption areas of the OH bands were converted to water contents ($C_{\text{H}_2\text{O}}$ in ppm by weight of H_2O) using the Beer-Lambert law in the form $C_{\text{H}_2\text{O}} = A_{\text{tot}}/I$, where I is the specific integral absorption coefficient of $15.3 \pm 0.7 \text{ ppm}^{-1} \text{ cm}^{-2}$ calibrated for feldspars¹⁹ (Table S1). Note that this calibration for plagioclase used here includes 7 data points of plagioclase, sanidine and microcline and there is scatter in the fitting¹⁹. If only the single point for plagioclase (GRR1968, with anorthite content of 94%, similar to lunar plagioclase with that of $\sim 97\%$)¹⁹ is used to calibrate the specific integral absorption coefficient, the coefficient is $8.0 \text{ ppm}^{-1} \text{ cm}^{-2}$ and the water content of plagioclase from 60015 (98.5 cm^{-2} of total absorbance area; Table S1) is 12.3 ppm. If only the 4 points for various plagioclase crystals are used for calibration, then the specific integral absorption coefficient is $10.7 \text{ ppm}^{-1} \text{ cm}^{-2}$ and the water content of plagioclase from 60015 is 9.2 ppm. For the paper, we use the published values (using the 7 data points of plagioclase, sanidine and microcline), so our results may represent minimum values.

The FTIR detection limit for water in plagioclase used in this study was determined using the signal variability (3σ) in the FTIR spectra ($3700 - 3100 \text{ cm}^{-1}$) in which no OH band could be detected. The detection limit thus determined is 0.46 ± 0.22 (1σ) ppm in terms of water, which is consistent with that of < 1 ppm typically given in the literature²². The propagated uncertainty on the measured water contents is $\sim 50\%$ (1σ), due to uncertainties in the OH band area determination based on manually drawn baselines, the uncertainties on the absorption coefficient (see discussion above) and thickness estimation (± 3 microns), and the fact that except for the 60015 plagioclase grain, three mutually perpendicular measurements could not be made, resulting in minimum water content estimates for each grain respectively. Even with this error, it is evident that there is detectable OH in plagioclase from the samples analyzed here.

3. Partition Coefficient between Plagioclase and Silicate Melt

In order to estimate the composition of a silicate melt in equilibrium with

plagioclase, a partition coefficient for the element of interest must be used. Partition coefficients are a function of temperature, pressure, melt composition, and plagioclase composition²³⁻²⁵. However, such dependence is not known, and only two empirically determined partition coefficients of hydrogen between plagioclase and silicate melt have been published in the literature²⁶. Both partition coefficients were established by comparing the water contents in phenocrysts and those in melt inclusions, but there is a difference of two orders of magnitude between these two values, 0.004 (ref. 27) versus 0.1 (ref. 28). In the first case, a linear function was established between water in plagioclase phenocrysts and that in plagioclase melt inclusions and 0.004 was calculated from this linear function²⁷. For the latter, however, the averages of water contents in plagioclase phenocrysts and plagioclase melt inclusions were used to calculate the partition coefficient (= 0.1) (ref. 28). As suggested by the authors²⁸, this partition coefficient may be meaningless because an average of water contents in melt inclusions, which had an order of magnitude of variation (410 – 3630 ppm H₂O), was used. Furthermore, a partition coefficient of 0.1 appears unrealistically high, being much higher than for typical nominally anhydrous minerals (~0.002 for olivine and ~0.02 for pyroxene)²⁹ but similar to that of apatite (0.1 – 0.25 (ref. 30), 0.13 – 0.85 (ref. 31)), a hydrous mineral. Therefore, we chose 0.004 as partition coefficient of H₂O between plagioclase and melt in this study. Note that the melt compositions for the estimated plagioclase-melt partition coefficient (0.004) are dacite to rhyolite³², which may not be ideal for lunar magma ocean composition, although this partition coefficient (0.004) has also been applied to terrestrial basalt³³.

References for Supplementary Information

1. Wilshire, H. G., Schaber, G. G., Silver, L. T., Phinney, W. C. & Jackson, E. D. Geologic setting and petrology of Apollo 15 anorthosite (15415). *Geol. Soc. Am. Bull.* **83**, 1083-1092 (1972).
2. McGee, J. J. Lunar ferroan anorthosites: Mineralogy, compositional variations, and petrogenesis. *J. Geophys. Res.* **98**, 9089-9105 (1993).
3. James, O. B. Lunar anorthosite 15415: Texture, mineralogy, and metamorphic history. *Science* **175**, 432-436 (1972).
4. Wasserburg, G. J., Papanastassiou, D. A. Age of an Apollo 15 mare basalts; lunar crust and mantle evolution. *Earth Planet. Sci. Lett.* **13**, 97-104 (1971).
5. Albarède, F. The recovery of spatial isotope distributions from stepwise degassing data. *Earth Planet. Sci. Lett.* **39**, 387-397 (1978).
6. Shearer, C. K. *et al.* Thermal and magmatic evolution of the Moon. *Rev. Mineral. Geochem.* **60**, 365-518 (2006).
7. Ganapathy, R., Morgan, J. W., Krähenbühl, U. & Anders, E. Ancient meteoritic components in lunar highland rocks: Clues from trace elements in Apollo 15 and 16 samples. *Proc. Lunar Sci. Conf.* **4**, 1239-1261 (1973).
8. Dixon, J. R. & Papike, J. J. Petrology of anorthosites from the Descartes region of the moon: Apollo 16. *Proc. Lunar Sci. Conf.* **6**, 263-291 (1975).
9. Hewins, R. H. & Goldstein, J. J. The provenance of metal in anorthositic rocks. *Proc. Lunar Sci. Conf.* **6**, 343-362 (1975).
10. Ebihara, M., Wolf, R., Warren, P. H. & Anders, E. Trace elements in 59 mostly highland Moon rocks. *Proc. Lunar Planet. Sci.* **22**, 417-426 (1992).

11. Mao, H. K. & Bell, P. M. Lunar metallic phase: Compositional variation in response to disequilibrium in regolith melting processes. *Proc. Lunar Sci. Conf.* **7**, 857-862 (1976).
12. Nunes, P. D., Tatsumoto, M., Knight, R. J., Unruh, D. M. & Doe, B. R. U-Th-Pb systematics of some Apollo 16 lunar samples. *Proc. Lunar Sci. Conf.* **4**, 1797-1822 (1973).
13. Dymek, R. F., Albee, A. L. & Chodos, A. A. Comparative petrology of lunar cumulate rocks of possible primary origin: Dunite 72415, troctolite 76535, norite 78235, and anorthosite 62237. *Proc. Lunar Sci. Conf.* **6**, 301-341 (1975).
14. Morgan, J. W., Ganapathy, R., Higuchi, H., Krähenbühl, U. & Anders, E. Lunar basins: Tentative characterization of projectiles, from meteoritic elements in Apollo 17 boulders. *Proc. Lunar Conf.* **5**, 1703-1736 (1974).
15. Premo, W. R. & Tatsumoto, M. U-Th-Pb, Rb-Sr, and Sm-Nd isotopic systematics of lunar troctolitic cumulate 76535: Implications on the age and origin of this early lunar, deep-seated cumulate. *Proc. Lunar Planet. Sci. Conf.* **22**, 381-397 (1992).
16. Lugmair, G. W., Marti, K., Kurtz, J. P. & Scheinin, N. B. History and genesis of lunar troctolite 76535 or: How old is old? *Proc. Lunar Sci. Conf.* **7**, 2009-2033 (1976).
17. Papanastassiou, D. A. & Wasserburg, G. J. Rb-Sr age of troctolite 76535. *Proc. Lunar Sci. Conf.* **7**, 2035-2054 (1976).
18. Rossman, G. R. Analytical methods for measuring water in nominally anhydrous minerals. *Rev. Mineral. Geochem.* **62**, 1-28 (2006).
19. Johnson, E. A. & Rossman, G. R. The concentration and speciation of hydrogen in feldspars using FTIR and ¹H MAS NMR spectroscopy. *Am. Mineral.* **88**, 901-911 (2003).
20. Johnson, E. A. & Rossman, G. R. A survey of hydrous species and concentrations in igneous feldspars. *Am. Mineral.* **89**, 586-600 (2004).
21. Miller, G. H., Rossman, G. R. & Harlow, G. E. The natural occurrence of hydroxide in olivine. *Phys. Chem. Miner.* **14**, 461-472 (1987).
22. Ingrin, J. & Blanchard, M. Diffusion of hydrogen in minerals. *Rev. Mineral. Geochem.* **62**, 291-320 (2006).
23. Bindeman, I. N., Davis, A. M. & Drake, M. J. Ion microprobe study of plagioclase-basalt partition experiments at natural concentration levels of trace elements. *Geochim. Cosmochim. Acta* **62**, 1175-1193 (1998).
24. Bédard, J. H. Trace element partitioning in plagioclase feldspar. *Geochim. Cosmochim. Acta* **70**, 3717-3742 (2006).
25. Hui, H., Oshrin, J. G. & Neal, C. R. Investigation into the petrogenesis of Apollo 14 high-Al basaltic melts through crystal stratigraphy of plagioclase. *Geochim. Cosmochim. Acta* **75**, 6439-6460 (2011).
26. Johnson, E. A. Water in nominally anhydrous crustal minerals: Speciation, concentration, and geologic significance. *Rev. Mineral. Geochem.* **62**, 117-154 (2006).
27. Johnson, E. A. Magmatic water contents recorded by hydroxyl concentrations in plagioclase phenocrysts from Mount St. Helens, 1980-1981. *Geochim. Cosmochim. Acta* **69**, A743 (2005).
28. Seaman, S. J., Dyar, M. D., Marinkovic, N. & Dunbar, N. W. An FTIR study of hydrogen in anorthoclase and associated melt inclusions. *Am. Mineral.* **91**, 12-20 (2006).

29. Hauri, E. H., Gaetani, G. A. & Green T. H. Partitioning of water during melting of the Earth's upper mantle at H₂O-undersaturated conditions. *Earth Planet. Sci. Lett.* **248**, 715-734 (2006).
30. McCubbin, F. M. *et al.* Nominally hydrous magmatism on the Moon. *Proc. Natl. Acad. Sci. U.S.A.* **107**, 11223-11228 (2010).
31. Boyce, J. W. *et al.* Lunar apatite with terrestrial volatile abundances. *Nature* **466**, 466-469 (2010).
32. Melson, W. G. Monitoring the 1980-1982 eruptions of Mount St. Helens: Compositions and abundances of glass. *Science* **221**, 1387-1391 (1983).
33. Hamada, M., Kawamoto, T., Takahashi, E., Fujii, T. Polybaric degassing of island arc low-K tholeiitic basalt magma recorded by OH concentrations in Ca-rich plagioclase. *Earth Planet. Sci. Lett.* **308**, 259-266 (2011).
34. Tera, F. & Wasserburg, G. J. Lunar ball games and other sports. *Lunar Sci.* **7**, 858-860 (1976).
35. Tatsumoto, M., Premo, W. & Unruh, D. M. Origin of lead from green glass of Apollo 15426: A search for primitive lunar lead. *J. Geophys. Res.* **92**, E361-E371 (1987).
36. Borg, L. E., Shearer, C. K., Asmerom, Y. & Papike, J. J. Prolonged KREEP magmatism on the Moon indicated by the youngest dated lunar igneous rock. *Nature* **432**, 209-211 (2004).
37. Papanastassiou, D. A. & Wasserburg, G. J. Rb-Sr ages of igneous rocks from the Apollo 14 mission and the age of the Fra Mauro formation. *Earth Planet. Sci. Lett.* **12**, 36-48 (1971).
38. Nyquist, L. E., Shih, C.-Y., Wooden, J. L., Bansal, B. M. & Wiesmann, H. The Sr and Nd isotopic record of Apollo 12 basalts: Implications for lunar geochemical evolution. *Proc. Lunar Planet. Sci. Conf.* **10**, 77-114 (1979).
39. Papanastassiou, D. A., Wasserburg, G. J. & Burnett, D. S. Rb-Sr ages of lunar rocks from the Sea of Tranquillity. *Earth Planet. Sci. Lett.* **8**, 1-19 (1970).
40. Tera, F., Papanastassiou, D. A. & Wasserburg, G. J. Isotopic evidence for a terminal lunar cataclysm. *Earth Planet. Sci. Lett.* **22**, 1-21 (1974).
41. Hauri, E. H., Weinreich, T., Saal, A. E., Rutherford, M. C. & Van Orman, J. A. High pre-eruptive water contents preserved in lunar melt inclusions. *Science* **333**, 213-215 (2011).
42. Saal, A. E. *et al.* Volatile content of lunar volcanic glasses and the presence of water in the Moon's interior. *Nature* **454**, 192-195 (2008).
43. Greenwood, J. P. *et al.* Hydrogen isotope ratios in lunar rocks indicate delivery of cometary water to the Moon. *Nature Geosci.* **4**, 79-82 (2011).

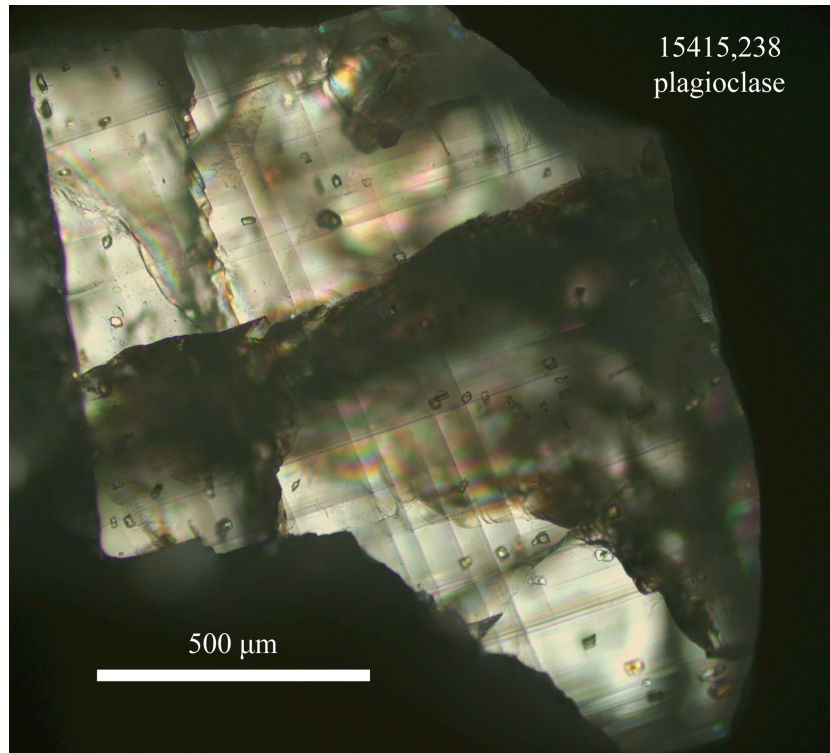


Fig. S1. Cross-polarized light image of plagioclase Grain 4 of FAN 15415,238. The thickness of this mineral section is 0.549 mm.

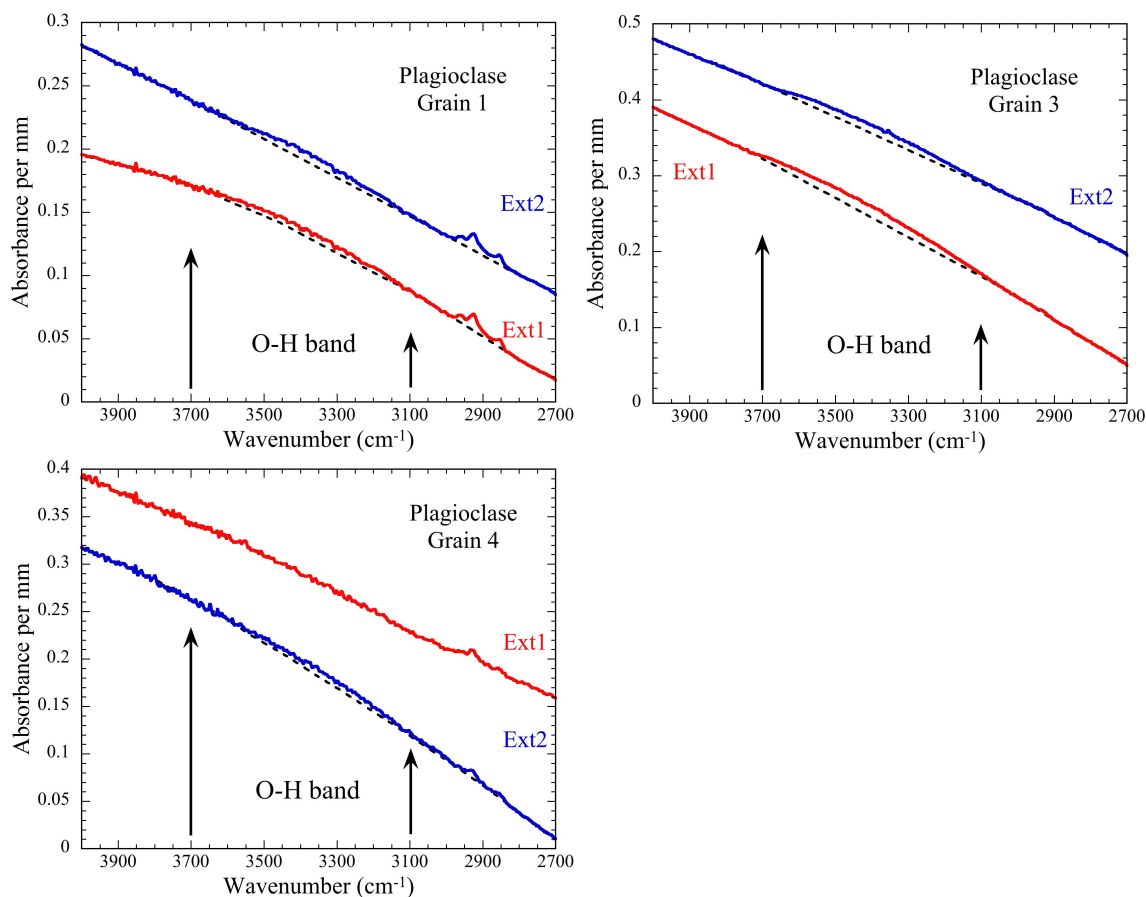


Fig. S2. Representative polarized FTIR spectra of plagioclase in FAN 15415,238 at mutually perpendicular orientations (Ext1 and Ext2). Spectra Ext1 and Ext2 in each crystal (Grain 1, 3 and 4) are from the same location for each grain. The broad band ($\sim 3700 - \sim 3100 \text{ cm}^{-1}$) in each spectrum is caused by O-H bond vibrations. The dashed line indicates the baseline position used for water content estimations. The small peaks between 3000 and 2800 cm^{-1} come from organic contamination on the mineral surface during sample preparation. Each spectrum is normalized to 1 mm.

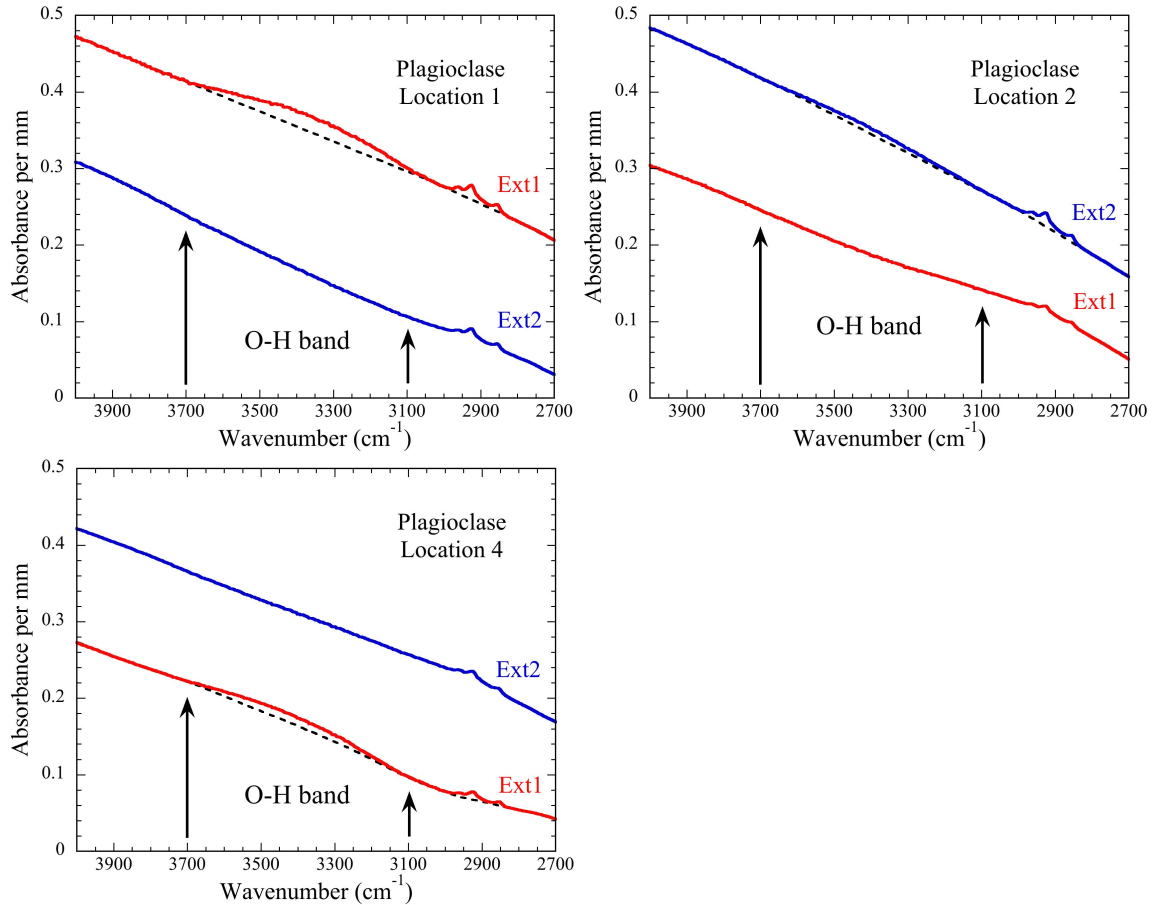


Fig. S3. Representative polarized FTIR spectra of plagioclase grain 1 in troctolite 76535,164 at mutually perpendicular orientations (Ext1 and Ext2). Spectra Ext1 and Ext2 in each plot (location 1, 2 and 4) were measured on the same spot on the plagioclase grains but with the infrared polarizer at two perpendicular orientations. Spectra Ext1 (or Ext2) at different locations may not be obtained with the same polarized infrared. The dashed line indicates the baseline position used for water content estimations. The small peaks between 3000 and 2800 cm⁻¹ come from organic contamination on the mineral surface during sample preparation. Each spectrum is normalized to 1 mm.

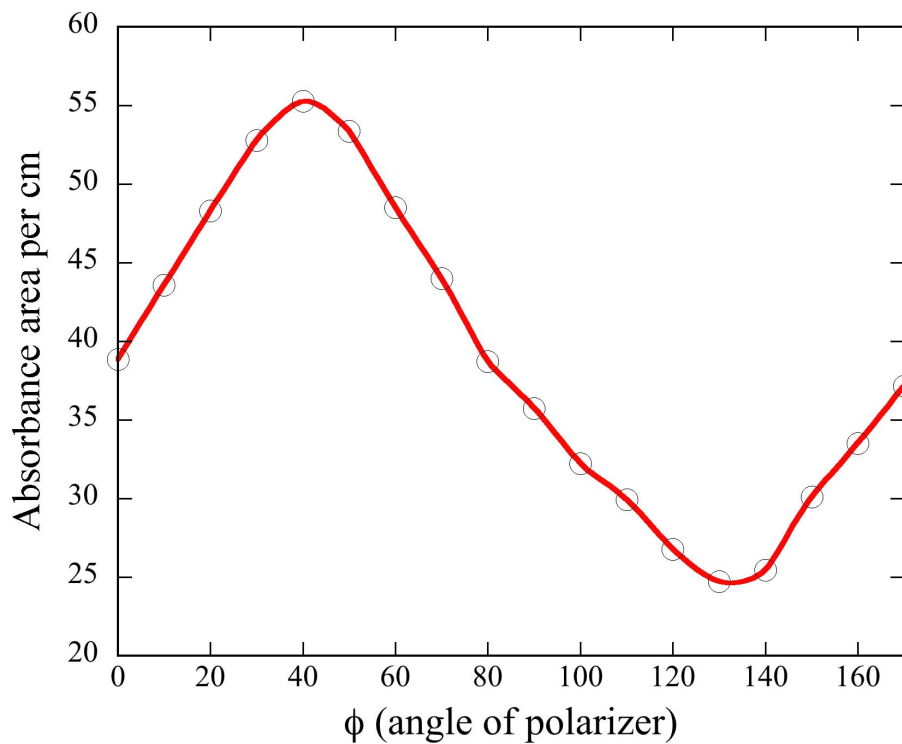


Fig. S4. Variation in OH absorbance area normalized to 1 cm with the angle of the infrared polarizer. FTIR measurements were performed at a single location on Grain 3 from FAN 15415,238. This plagioclase grain was not oriented relative to any major axis and its orientation was fixed during this series of measurements. Circles show the absorbance calculated as the area beneath the OH bands (~ 3700 to ~ 3100 cm^{-1}).

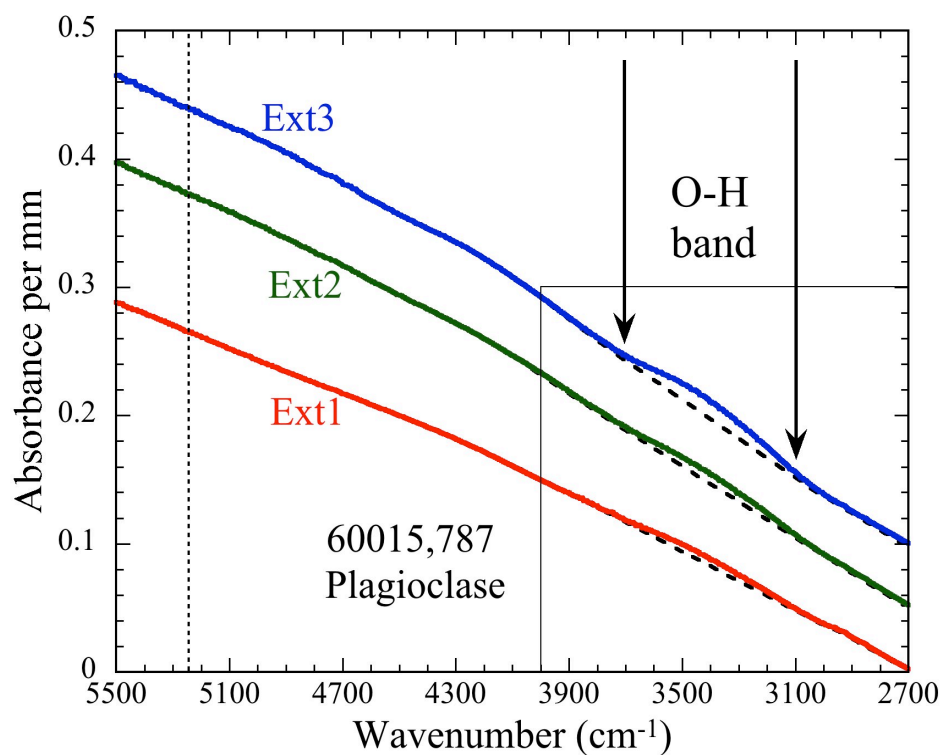


Fig. S5. Representative polarized FTIR spectra in the OH band region of FAN 60015 plagioclase. No bands were observed at $\sim 5240\text{ cm}^{-1}$ in all the plagioclase spectra in this study, which is consistent with that the $3700\text{-}3100\text{ cm}^{-1}$ bands are for hydroxyl species, not molecule water nor water in melt inclusions. The portions of spectra in the box are the same as those in Fig. 1b.

Table S1. Integrated OH absorbance values and water contents obtained from FTIR analyses of lunar plagioclases and olivines.

Sample	Grain	Location	Thickness (mm)	Ext1 band ^a area (cm ⁻²)	Ext2 band ^a area (cm ⁻²)	Ext3 band ^a area (cm ⁻²)	Total band ^a area (cm ⁻²)	Water ^b (H ₂ O ppm)
15415	Pl1 ^c	1	0.679	19.9	26.3		46.2	3.0
15415	Pl2 ^c	1	0.907	21.5	24.9			
		2	0.907	21.1	28.4			
		3	0.907	18.2	28.6			
		Average		20.3	27.3		47.6	3.1
15415	Pl3 ^c	1	1.021	41.6	30.7			
		2	1.021	42.2	34.1			
		3	1.021	44.8	29.2			
		4	1.021	48.1	28.5			
		5	1.021	49.2	32.8			
Average		45.2	31.1		76.2	5.0		
15415	Pl4 ^{c,d}	1	0.549	n.d. ^f	6.4			
		2	0.549	n.d. ^f	8.6			
		3	0.549	n.d. ^f	8.3			
		Average			7.8		7.8	0.5
60015	Pl	1	1.061		26.5	58.6		
		2	1.061		29.5	50.1		
		3	1.061		22.1	55.9		
		4	1.061		26.2	58.7		
		5	1.641	14.8	22.1			
		6	1.641	18.7	23.7			

		7	1.641	17.5	29.3		
		8	1.641	16.2	27.9		
		Average		16.8	25.9	55.8	98.5
							6.4
76535	P11 ^{c,e}	1	1.086	41.7	n.d. ^f	41.7	2.7
		2	1.086	n.d. ^f	13.0	13.0	0.8
		3	1.086	n.d. ^f	41.1	41.1	2.7
		4	1.086	37.4	n.d. ^f	37.4	2.4
76535	P12 ^c		1.194	n.d. ^f	n.d. ^f		
76535	P13 ^c		1.346	n.d. ^f	n.d. ^f		
76535	P14 ^c		0.796	n.d. ^f	n.d. ^f		
76535	O11 ^c		1.055	n.d. ^f	n.d. ^f		
76535	O12 ^c		0.604	n.d. ^f	n.d. ^f		

- a) Area of integrated absorbances presented here are for spectra normalized to 1 cm and at mutually perpendicular orientations (Ext1, Ext2, Ext3) of the infrared polarizer relative to the grain.
- b) The 1σ uncertainty on the measured water content is ~50% (see supplementary information).
- c) We could only obtain spectra at two mutually perpendicular orientations. Therefore, the water content shown here (or location for P11 of 76535,164) represents a minimum value.
- d) OH was detected at only one of the two orientations probably because the grain section was too thin (0.549 mm).
- e) The highly variable total band area of this grain (P11) may be in part due to the fact that it is a plagioclase crystal aggregate. Location 1, 3 and 4 were analyzed at the same sample orientation, but different from one for location 2 during FTIR measurements.
- f) n.d. = no OH bands observed in the infrared spectra.

Table S2. Water concentrations in the source regions of lunar basalts for which indigenous water has been measured and their isochron ages.

Sample	Age ^a Ga	Parental melt ^b Water ppm	3% partial melting ^c Water in source ppm	20% partial melting ^c Water in source ppm
74220	3.48 (Pb-Pb)	615 – 1410	18.45 – 42.3	123 – 282
15427	3.41 (Pb-Pb)	260 – 745	7.8 – 22.35	52 – 149
NWA 2977	2.86 (Sm-Nd)	360 – 850	10.8 – 25.5	72 – 170
14053	3.96 (Rb-Sr)	71 – 200	2.13 – 6	14.2 – 40
12039	3.19 (Rb-Sr)	120 – 756	3.6 – 22.68	24 – 151.2
10044	3.71 (Rb-Sr)	106 – 156	3.18 – 4.68	21.2 – 31.2
75055	3.77 (Rb-Sr)	~ 134	~ 4.02	~ 26.8

a) The ages for the basalts are isochron ages and come from literature data: 74220³⁴, 15427³⁵, NWA 2977³⁶, 14053³⁷, 12039³⁸, 10044³⁹ and 75055⁴⁰. Isotopic dating systems used are shown in parentheses.

b) The water concentrations in parental melts of these basalts are based on literature data: 74220⁴¹, 15427⁴², NWA 2977³⁰, 14053^{42,43}, 12039⁴³, 10044⁴³ and 75055⁴³.

c) The water concentrations in the source regions assuming 3% or 20% partial melting to form the parental melts of these basalts.